Computers & Graphics (2019)

Contents lists available at ScienceDirect

Computers & Graphics

journal homepage: www.elsevier.com/locate/cag

Real-time non-photorealistic animation for immersive storytelling in "Age of Sail"

Cassidy Curtis[a], Kevin Dart[b], Theresa Latzko[b], John Kahrs[c]

[a]*Google Spotlight Stories*
[b]*Chromosphere LA*
[c]*Boathouse Studios*

ARTICLE INFO

Article history:
Received October 21, 2019

Keywords: non-photorealistic rendering, real-time, virtual reality, storytelling, animation

ABSTRACT

Immersive media such as virtual and augmented reality pose some interesting new challenges for non-photorealistic animation: we must not only balance the screen-space rules of a 2D visual style against 3D motion coherence, but also account for stereo spatialization and interactive camera movement, at a rate of 90 frames per second. We introduce two new real-time rendering techniques: MetaTexture, an example-based texturing method that adheres to the movement of 3D geometry while preserving the texture's screen-space characteristics, and Edge Breakup, a method for roughening edges by warping with structured noise. We also describe a custom rendering pipeline featuring art-directable coloring, shadow filtering, and texture indication, and our approach to animating and rendering a painterly ocean in real time. We show how we have used these techniques to achieve the "moving illustration" style of the real-time immersive short film "Age of Sail".

1. Introduction

The immersive short film *Age of Sail* [1] tells the story of an old sailor adrift in the north Atlantic in the year 1900. For this story to succeed, it had to reach the audience on two levels: engage them emotionally with the characters, but also immerse them in a world that is believable enough to create a real sense of peril. The story also had to run in real time within the limitations of current virtual reality hardware, including mobile devices.

We chose a visual style that we felt would support these goals: deliberately polygonal shapes with naturalistic proportions and movement, coupled with a limited color palette, flat-colored regions with roughened edges, rounded shadow shapes, and indications of texture (see Figures 1-2).

Adapting even a simple visual style from a static flat image to real-time animated 6DoF VR is an act of interpretation that requires careful thought. In this paper we will describe how we captured the essential qualities of *Age of Sail's* visual style, including two new rendering techniques (MetaTexture and Edge Breakup) that solve problems unique to the 6DoF VR context.

1.1. Related Work

Balancing screen-space stylistic rules against 3D motion coherence is a well-known challenge in the field of NPAR. Various approaches have been made to produce coherent silhouettes [2, 3, 4, 5], using brushstrokes to fill regions [6, 7], volumetric textures [8] and screen-space advection [9, 10]. Our method differs from most of these in that it can be implemented within an existing real-time animation and rendering pipeline, using only a few custom shaders and image-processing filters. Also, none of these previous methods account for the needs of stereoscopic 6DoF VR. The artifacts they introduce may differ between left and right eye views, resulting in a misleading or incoherent perception of stereo depth.

There have been various papers describing non-photorealistic rendering in VR or AR: [11, 12, 13, 14, 15]. However, none of these address the complete set of issues including stereo fusion and temporal coherence. Northam et al [16] does address stereo coherence, but uses a technique inappropriate for real-time rendering.

Our multresolution texture method can be considered a gen-

Fig. 1: Concept art for *Age of Sail* by Céline Desrumaux and Jasmin Lai.

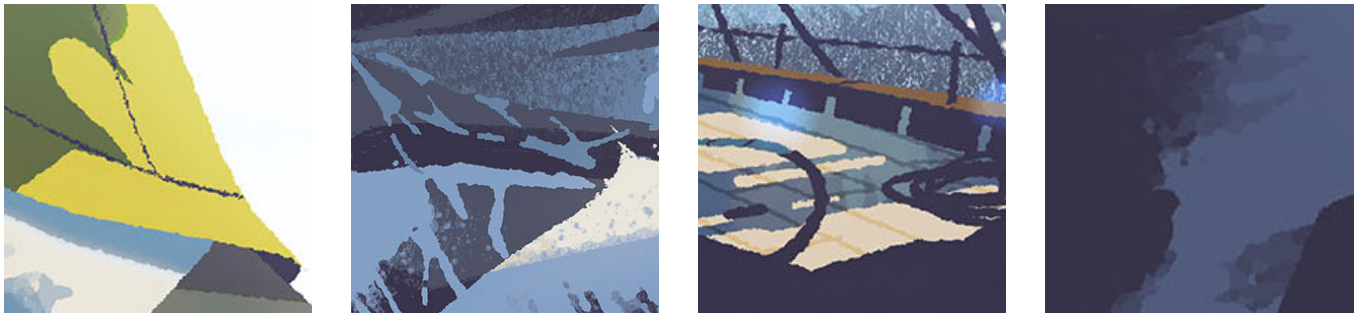

(a) rough edges (b) limited color palette (c) rounded shadow shapes (d) indications of texture

Fig. 2: Important details from the concept art.

eralization of the UV-gradient-based curved hatching described by Saito and Takahashi [17]. Multiresolution or self-similar textures have been used to allow screen-space marks to adjust smoothly under changes in viewpoint, scale, or deformation: Bénard et al [18] and Kalnins et al [2] do it in linear edge space; Klein et al [11] rely on pre-rendered "art maps" that do not account for real-time lighting or animation changes. Dirksen [19] used a scalar multiresolution noise texture for pixel-scale dithering in 6DoF VR. Our method is more general, operating on full-color textures as well as vector fields, with special considerations for screen space orientation, texture skewing, and continuity across triangle edges.

Our edge breakup method is a direct extension of the warping technique used on the immersive short *Pearl* [20], with additional features specific to the 6DoF VR domain. Our overall approach to planning and executing non-photorealistic animation production follows the guidelines set out by Curtis [21].

This paper is an extended journal version of the Expressive 2019 paper by Curtis et al [22]. Compared to the original paper, the major new contributions in this version are: (1) analysis of the concept art that motivated the development of these techniques, (2) a detailed explanation of the custom rendering pipeline, ocean, and shaders, and (3) a method for compensating for contrast reduction in MetaTexture.

1.2. Overview

We will start by describing our overall artistic design approach (Section 2), and the new non-photorealistic techniques MetaTexture (Section 3), and Edge Breakup (Section 4). We will describe the customized animation and rendering pipeline (Section 5) that we built around these techniques. Following that, we will show examples of how we applied these techniques in production (Section 6), and suggest future directions for further exploration (Section 7).

2. Design

2.1. Inspiration

Age of Sail's visual style (Figure 1) is inspired by the work of painters like Bernie Fuchs [23] and Thomas Hoyne [24]. Fuchs uses limited color palettes with roughened edges and hints of texture to produce evocative scenes; some of his paintings also have an "inner glow" that comes from his unique oil rub-out technique (see Figure 3). Hoyne's compelling portrayals of life on the open ocean show thoughtful control of texture in lit and shadowed regions.

Fig. 3: Oil painting *Ship in Green Water* by Bernie Fuchs. Note the darkened edges that give the scene a subtle "inner glow" effect.

A key insight we drew from these illustrators is that each in his own way controls what the audience perceives by manipulating the salience of every element in the scene. They use techniques like *indication* [25] to convey the feeling that an object is textured without explicitly rendering its texture everywhere in full detail, or *lost and found edges* [26] which focuses

Fig. 4: A final rendered frame from *Age of Sail*.

the viewer's attention by carefully planning the locations of the most salient edges, and reducing edge salience elsewhere. What these techniques have in common is that they *remove information* from the scene, engaging and inviting the viewer to fill in the blanks.

2.2. Our design choices

We used a combination of these approaches in our designs. The hand-painted concept art in Figure 1 illustrates several of the elements of *Age of Sail*'s visual language. The scene consists mainly of solid-colored regions which, though simple and polygonal in shape, are drawn with rough edges that give them a handmade quality (Figure 2a). The color palette is limited: for example, there are only four shades of blue in the ocean (Figure 2b). Shadow shapes are rounded in a way that unifies the overall composition, and suggests they were painted with a brush of a certain size (Figure 2c). Texture is indicated sparingly, mainly on transitions between the lit and shadowed regions of smooth surfaces (Figure 2d).

The choice to build the image mainly of regions of solid color unifies the overall composition in an appealing way, and also makes the production process more flexible. Because overlapping objects with matching colors are perceived as one shape, the digital artists on our team are free to mix different techniques to produce a seamless end result (Figure 4).

2.3. The devil in the details

If our design style consisted only of simple, smooth-edged regions of color, adapting it to an immersive medium like 6DoF VR would be fairly straightforward. However, our style also has some highly salient fine-grained detail, of two distinct kinds: texture, and rough edges. These details pose an interesting technical challenge.

To function well in VR, every detail in the scene must (1) conform to the 2D screen-space rules of the style, (2) cohere with the movement of objects in 3D space, (3) adapt to the audience's dynamically changing viewpoint, and (4) spatialize stereoscopically at an appropriate depth. This is a highly overconstrained problem.

Fortunately, our goal is not a mathematically perfect solution, but an *illusion* that achieves all of these goals *in the viewer's mind* (a problem analogous to the "plausible physics" proposed by Barzel et al [27].) An error that is imperceptible to the audience is equivalent to a perfect result for our purposes. Our task, then, is to develop methods whose mistakes can be pushed below the threshold of perceivability. We will describe two such methods in the sections that follow: MetaTexture (Section 3) and Edge Breakup (Section 4).

3. MetaTexture

To achieve the illusion of a 2D visual style in 6DoF VR, we need a texturing technique that preserves the style's screen-space characteristics while adhering to the movement of surfaces in 3D space. The technique must also be simple enough to perform well at high frame rates, a requirement that excludes most procedural or solid texturing methods. For this reason, we have opted for an example-based approach.

A *MetaTexture* is a multiresolution texture made by blending multiple copies of a single tileable example texture (Figure 5a),

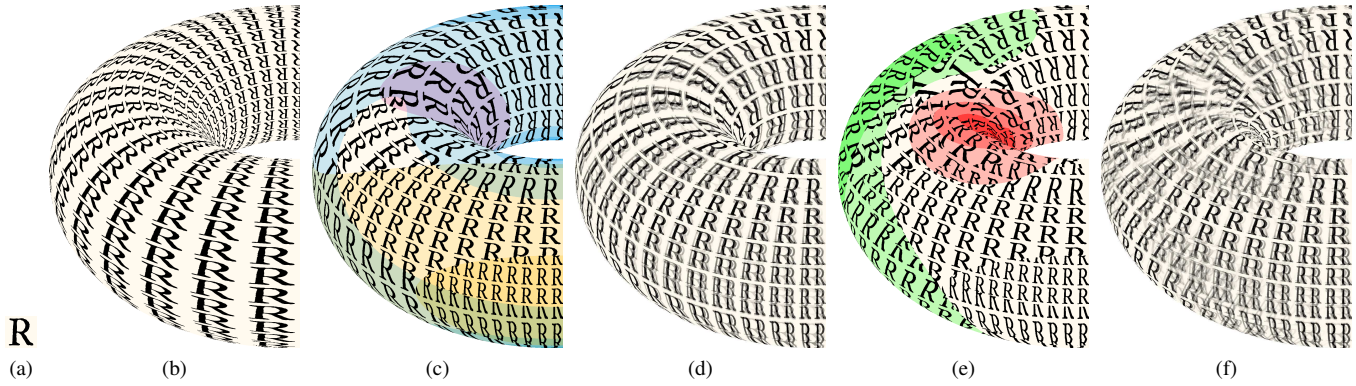

Fig. 5: (a) Example texture. (b) Ordinary texture mapping produces undesirable distortion in screen space. (c) Quantized regions with UV scales adjusted to the nearest power-of-two, to approximate screen-space size of example texture. (d) MetaTexture with blending. (e) Quantized regions of positive (green) or negative (red) skew ($n = 4$). (f) MetaTexture with skew compensation and blending.

under different affine transformations in UV space. The transforms are chosen so that at any point on the surface, the transformed textures approximate as closely as possible the example texture's shape and size in screen space (Figure 5c). Although the range of possible transforms is infinite, only a finite number of transforms are needed for any given fragment, so the texture can still be calculated in constant time.

3.1. Texture scales and blend coefficients

The first component of the affine transformation is the scale of the texture in UV space, which may be non-uniform. One way to determine texture scales is by using the magnitudes of the screen-space gradients of the texture coordinates $\vec{U} = \langle u, v \rangle$. Assuming a square example texture of width w pixels, the ideal texture scale, i.e. one which would produce locally the same screen-space proportions of the original texture, would be:

$$\vec{S} = \left\langle \frac{1}{w|\nabla u|}, \frac{1}{w|\nabla v|} \right\rangle \tag{1}$$

However we cannot simply scale the texture by this vector locally at every pixel, as these gradients may vary continuously across the screen, producing wildly distorted textures. We must find a discrete set of scale values that can be relied upon not to change, and then smoothly interpolate between the resulting textures. For this, we have chosen the powers of two (similar to anisotropic mipmaps or ripmaps). We convert the scale to an exponent vector $\vec{E}$ as follows:

$$\vec{E} = \left\langle \log_2(\vec{S}_u), \log_2(\vec{S}_v) \right\rangle \tag{2}$$

We threshold those exponents to produce the four nearest power-of-two scaled texture coordinates $\vec{U}_{0-3}$, and blend coefficients $\vec{B}$:

$$\vec{U}_0 = \left\langle 2^{\lfloor E_u \rfloor} u, 2^{\lfloor E_v \rfloor} v \right\rangle \tag{3}$$

$$\vec{U}_1 = \langle 2u_0, v_0 \rangle \tag{4}$$

$$\vec{U}_2 = \langle u_0, 2v_0 \rangle \tag{5}$$

$$\vec{U}_3 = \langle 2u_0, 2v_0 \rangle \tag{6}$$

$$\vec{B} = \langle \beta(E_u - \lfloor E_u \rfloor), \beta(E_v - \lfloor E_v \rfloor) \rangle \tag{7}$$

where $\beta(x)$ is any smooth monotonic blending function meeting the criteria that $\beta(0) = 0$ and $\beta(1) = 1$. (In practice, we have found the cubic blend $\beta(x) = -2x^3 + 3x^2$ produces pleasing results.)

The MetaTexture color M is then determined by sampling the texture T four times, and blending the results:

$$\begin{aligned} M(\vec{U}) = (1 - B_v)[(1 - B_u)T(\vec{U}_0) + B_u T(\vec{U}_2)] + \\ B_v[(1 - B_u)T(\vec{U}_1) + B_u T(\vec{U}_3)] \end{aligned} \tag{8}$$

Because the blend function is smooth, it is not immediately obvious to the viewer where one texture scale region ends and the next one begins (see Figure 5d). The regions overlap, and the transitions between them are less salient than the details of the texture itself, and thus they fall below the threshold of perceivability. This is also true of how the texture changes when an animated surface moves through 3D space: the transitions over time are quite subtle compared to the gross movement of the object as a whole. Thus we preserve the twin illusions of consistent 2D texture quality and 3D motion coherence while minimizing distracting artifacts.

3.2. Approximate smooth UV gradients

UV gradients have two disadvantages: first, they may not be continuous at triangle boundaries, which can lead to visible hard-edged artifacts when the discontinuities are large (see Figure 6a.) Second, gradients are based on derivatives, which must be calculated in the fragment shader, which is less efficient than the vertex shader when triangles are large.

We can approximate the UV gradients by deriving them from the local tangent and binormal, which can be calculated in the vertex shader and interpolated smoothly across the triangles. Given the screen-space projections of the unit tangent and binormal ($\vec{T}_s$ and $\vec{B}_s$), and the world-space UV gradients $\nabla_w u$ and $\nabla_w v$, we approximate the screen-space gradients as follows:

$$\nabla_s u = |\nabla_w u|\vec{T}_s/|\vec{T}_s|^2 \tag{9}$$

$$\nabla_s v = |\nabla_w v|\vec{B}_s/|\vec{B}_s|^2 \tag{10}$$

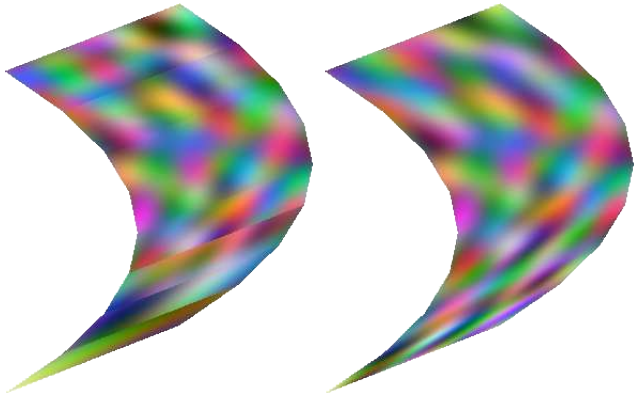

(a) (b)

Fig. 6: (a) hard-edged artifacts resulting from discontinuous UV gradients. (b) approximate smooth gradients.

By substituting $\nabla_s u$ and $\nabla_s v$ into Equation 1, we obtain smoother results, as seen in Figure 6b.

Note: this method assumes the world-space UV gradients are known for any vertex in the mesh. Calculating those gradients for every vertex every frame on deforming meshes may be computationally expensive on certain hardware configurations. In practice we have only used this method on meshes where the gradients can be approximated by a constant value across the entire mesh. (This method also assumes that the gradients of u and v are perpendicular in world space, which may not be true on all meshes. This is only an issue if compensating for skew as described in Section 3.4.)

Under certain circumstances, the method described above might produce a stereoscopic "shimmer" artifact, where the left and right eye views have completely unrelated textures when a surface subtends significantly different areas in the two different views. This can be corrected by projecting $\vec{T}_s$ and $\vec{B}_s$ using a single camera rather than projecting each eye separately. (In practice we have not found this necessary, since this only occurs when a large vertical surface is oblique to camera, and our most prominent use of MetaTexture is on the horizontal surface of the ocean: see Section 6.1.)

3.3. Compensating for radial angle

The above calculations assume that the desired result is a uniform texture scale in screen space. However, in a VR device, pixels near the edge of the screen subtend a significantly smaller radial angle than pixels near the center, which means that the *apparent* level of detail varies across the screen. Thus, the same surface will have a different appearance when viewed head-on versus obliquely, a difference that is quite noticeable if the viewer turns her head. We compensate for this by adding a radial angle compensation coefficient α to equation 1:

$$\vec{S} = \left\langle \frac{1}{\alpha w |\nabla u|}, \frac{1}{\alpha w |\nabla v|} \right\rangle \tag{11}$$

As a pixel's radial angle depends on its location and the camera's focal length, we can derive α from the screen space position s and the camera projection matrix P as follows:

$$\vec{Q} = \left\langle \frac{s_x}{P_{0,0}}, \frac{s_y}{P_{1,1}} \right\rangle \tag{12}$$

$$\alpha = |\vec{Q}|^2 + 1 \tag{13}$$

3.4. Compensating for skew

So far we have only discussed scaling textures orthogonally along the u and v axes. However, it is still possible for textures to become highly stretched or distorted if the angle between ∇u and ∇v diverges too far from 90 degrees (Figures 7a and 5d).

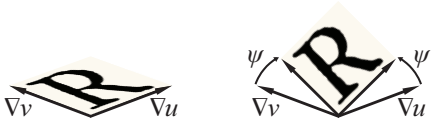

(a) (b)

Fig. 7: (a) Skewed texture. (b) Compensating for skew by rotating the eigenvectors in UV space.

To compensate for this distortion, we can rotate both eigenvectors in UV space by an angle ψ so that their screen-space projections become perpendicular (Figure 7b). To find ψ, we start by computing a *skew* factor σ as follows:

$$\sigma = \tan^{-1}(\epsilon)\left(\frac{\nabla u}{|\nabla u|} \cdot \frac{\nabla v}{|\nabla v|}\right) \tag{14}$$

where

$$\epsilon = \begin{cases} |\nabla u|/|\nabla v|, & \text{if } |\nabla u| \le |\nabla v| \\ |\nabla v|/|\nabla u|, & \text{otherwise} \end{cases} \tag{15}$$

We quantize the skew factor at a user-determined finite number of levels n (see Figure 5e; in practice, values between 2 and 4 seem to work well) and use those to calculate quantized angles ψ_0, ψ_1, and finally determine new UV coordinates $\vec{U}'$, $\vec{U}''$:

$$\sigma_0 = \frac{\lfloor n\sigma \rfloor}{n} \tag{16}$$

$$\sigma_1 = \frac{\lfloor n\sigma \rfloor + 1}{n} \tag{17}$$

$$\psi_0 = \tan^{-1}\left(\frac{\sigma_0}{2}\right) \tag{18}$$

$$\psi_1 = \tan^{-1}\left(\frac{\sigma_1}{2}\right) \tag{19}$$

$$\vec{U}' = \langle u\cos(\psi_0) + v\sin(\psi_0), v\cos(\psi_0) + u\sin(\psi_0)\rangle \tag{20}$$

$$\vec{U}'' = \langle u\cos(\psi_1) + v\sin(\psi_1), v\cos(\psi_1) + u\sin(\psi_1)\rangle \tag{21}$$

Quantizing and blending based on the skew factor means we must sample the texture eight times rather than four. We generate the eight sets of coordinates $\vec{U}'_{0..3}$ and $\vec{U}''_{0..3}$ using equations 2-5, and we calculate a third blend factor B_w, and MetaTexture as follows:

$$B_w = \beta(n\sigma - \lfloor n\sigma \rfloor) \tag{22}$$

$$\begin{aligned} M(\vec{U}) = (1 - B_w)\{(1 - B_v)[(1 - B_u)T(\vec{U}'_0) + B_u T(\vec{U}'_2)] + \\ B_v[(1 - B_u)T(\vec{U}'_1) + B_u T(\vec{U}'_3)]\} + \\ B_w\{(1 - B_v)[(1 - B_u)T(\vec{U}''_0) + B_u T(\vec{U}''_2)] + \\ B_v[(1 - B_u)T(\vec{U}''_1) + B_u T(\vec{U}''_3)]\} \end{aligned} \tag{23}$$

There is a tradeoff here: the reduced distortion comes at the cost of increasing the number of overlapping regions (Figure 5f). In practice, whether skew compensation is needed depends on the texture and the desired result.

3.5. Orienting texture to indicate contour

In some cases a texture may have a clear sense of directionality to it, which you may wish to use to indicate contour along the surface. In this case we can reorient the texture depending on the relative magnitudes of ∇u and ∇v. (See Figure 8.)

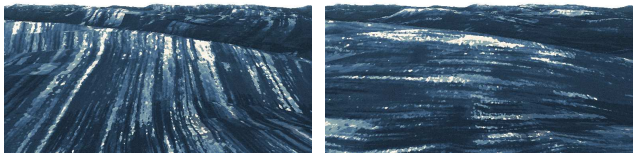

(a) (b)

Fig. 8: An ocean surface with a clearly directional MetaTexture (a) in its default orientation, (b) re-oriented to indicate contour.

3.6. Compensating for contrast reduction

The above techniques alone do not guarantee a consistent level of contrast across the entire image. Some regions may be dominated by a single texture (Figure 9a) while others may be a blend of up to eight different textures (Figure 9b), which significantly reduces feature contrast and salience. (A similar problem often occurs in "fractalized" textures [28].)

This can be improved by using a histogram-preserving blending operator as described by Heitz and Neyret [29]. If you start with a texture that already has an approximately Gaussian histogram (Figure 9d), which turns out to be quite common in noise-based textures, you can skip the gaussification and degaussification steps entirely, and simply multiply the contrast by a single compensation factor c, which can be reduced to the simple function:

$$c = k(B_u)k(B_v)k(B_w) \tag{24}$$

where

$$k(t) = 2t^2 - 2t + 1 \tag{25}$$

The adjusted result will more closely approximate the apparent contrast level of the original texture (Figure 9c). Note: while this feature was not needed in the case of *Age of Sail*, we have since found it useful on other projects where the reduced contrast is more noticeable.

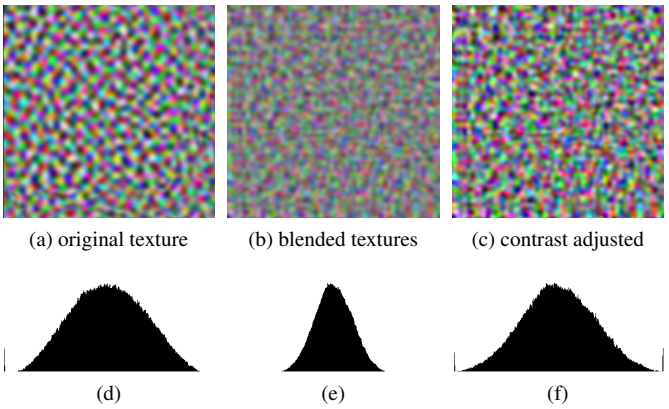

(a) original texture (b) blended textures (c) contrast adjusted

(d) (e) (f)

Fig. 9: (a/d) Original texture and its histogram. (b/e) Blending multiple textures reduces contrast. (c/f) A histogram-preserving blend restores contrast.

4. Edge Breakup

The rough edges in the concept art (Figure 2a) were made using standard digital painting techniques, which typically involve 2D height fields or halftone patterns. To reproduce the look of those edges in stereoscopic 3D, we need to create the illusion that the roughness is "attached" to 3D objects in the scene. To achieve this, we use the strategy of warping the image with a structured vector field.

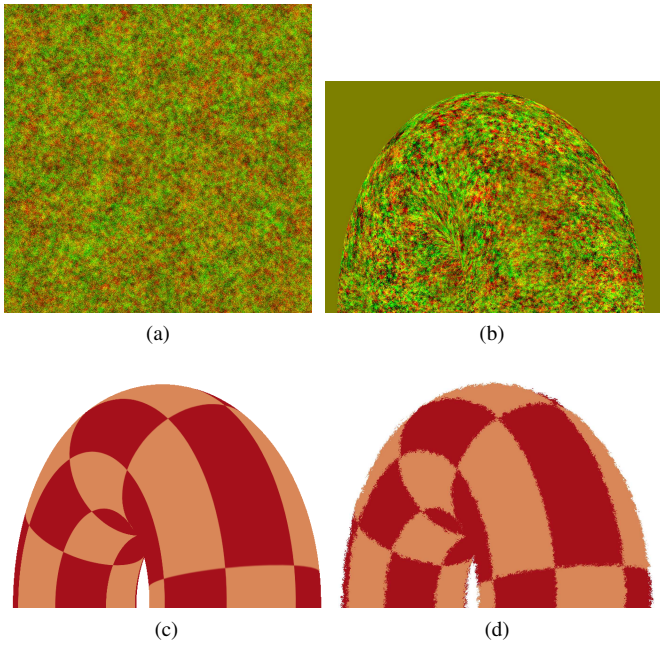

(a) (b)

(c) (d)

Fig. 10: (a) A self-similar, tileable noise texture. (b) Warp pass, with noise rendered with MetaTexture on inflated surface. (c) Color pass, with clean-edged rendered surface. (d) Edges roughened by warping.

We start with a texture that represents warp vectors using the red and green color channels. (For best results, the texture should tile seamlessly and be self-similar, as in Figure 10a). To "attach" this texture to a 3D object, we map it onto the object's geometry, and render it using different shaders into a separate buffer (Figure 10b). This screen-space vector field is then used

to warp the clean-edged color pass (Figure 10c) to produce the final result (Figure 10d). Because the vector field is coincident with the geometry in 3D space, it will always move coherently, and its salient features will also spatialize at the correct depth when viewed in binocular stereo. This way we avoid the undesirable "rippled glass" effect common with image warping effects.

With an ordinary texture, the perceptual quality of the warped edge may vary depending on the viewer's point of view. For example, when viewed up close, the texture may get blurry, resulting in lines that are soft and wiggly as opposed to rough. (This is in fact what happens in the 6DoF version of the immersive short *Pearl* [20].) So we use MetaTexture here as well, to guarantee that the roughness remains perceptually consistent regardless of the viewer's point of view.

4.1. Edge inflation

To ensure that the edges can be warped in both directions, both towards and away from the object's silhouette, our shader inflates the geometry by a small amount (measured in screen space, as pixels or as percentage of image size) by moving each vertex outward along its screen-space projected normal. (See Figure 11.)

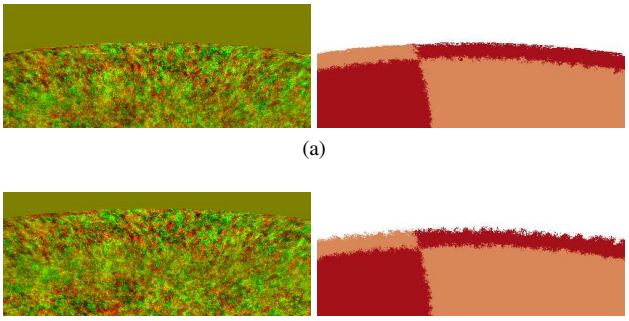

(a)

(b)

Fig. 11: The effect of edge breakup (a) without inflation and (b) with inflation. Note that without inflation, the edge breakup affects only pixels that are entirely within the object's silhouette, resulting in a hard outer edge.

4.2. Animated line boil

Line boil is how animators describe the subtle differences between drawn lines across successive frames of hand-drawn animation. We can mimic this effect by adding a periodically changing offset to the texture coordinates. (See Figure 12.)

Fig. 12: Four frames from a scene with animated line boil.

4.3. Compensating for camera roll

Because the red and green channels encode warp vectors in screen space, if we were to roll the camera (e.g. if the viewer tilts her head sideways), the warped edges would change their shape (see Figure 13.) To compensate for this, we rotate the vectors in the shader, so that the frame of reference remains aligned with the screen space U gradient regardless of orientation.

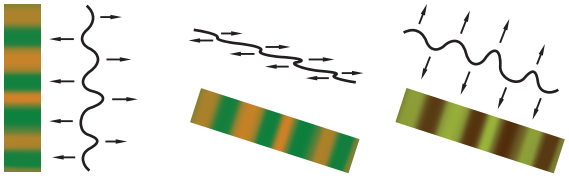

(a) (b) (c)

Fig. 13: (a) Warping an edge using vectors encoded in the red/green channels. (b) Warping with the same vectors after camera rotation produces a different shape. (c) Rotating the vectors before encoding keeps the shape consistent.

4.4. Compensating for distance

The above techniques will ensure a uniform degree of screen-space roughness, creating the illusion that the entire image was painted using the same tools and materials. However, in order to preserve certain important details, it is sometimes desirable to reduce the roughness as an object recedes in the distance. In that case we can attenuate the intensity of the warp effect ρ based on the distance from camera d:

$$\rho' = \frac{\rho}{1 + d^2} \tag{26}$$

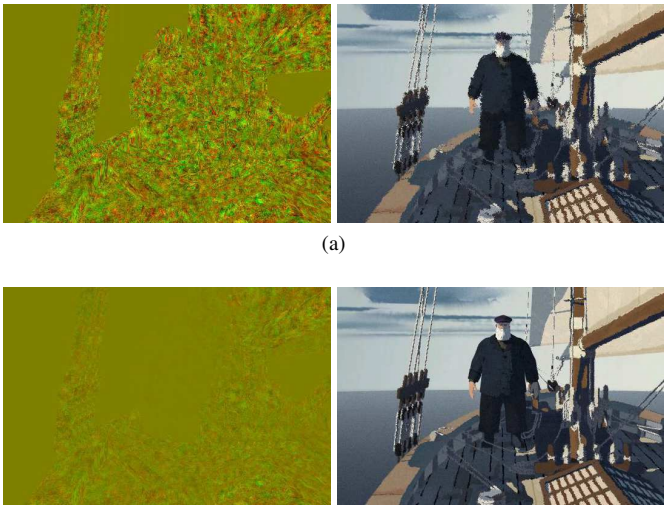

(a)

(b)

Fig. 14: The effect of edge breakup (a) without and (b) with distance compensation. Note that without distance compensation, the edge breakup makes the character's silhouette more difficult to read.

5. The Rendering Pipeline

To render the full scene with our visual style, we do not need all of the features of a traditional photorealistic renderer, but we do need some extra rendering passes and image processing filters not typically present in standard pipelines. So we developed a custom rendering pipeline comprising the minimal set of features we needed, optimized for real-time performance (see Figure 15).

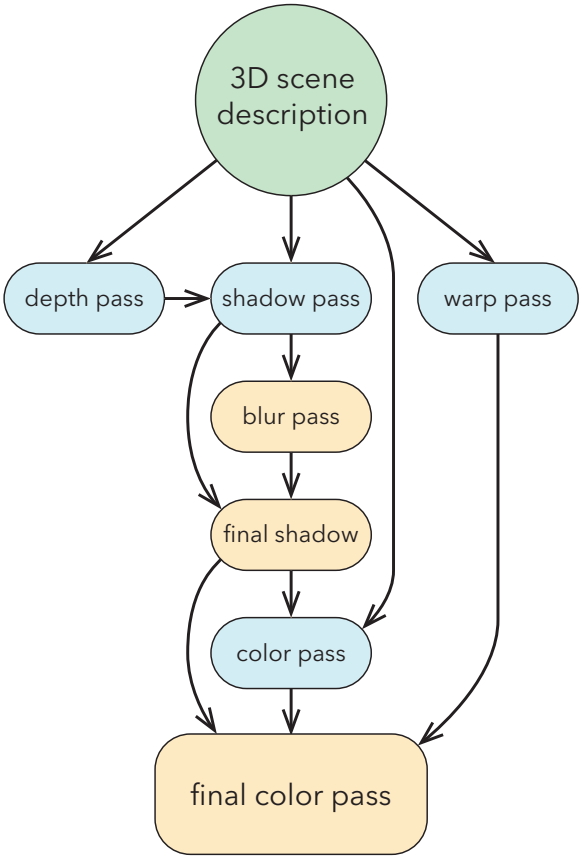

Fig. 15: Our custom rendering pipeline, showing the dependencies between the different passes. (Blue indicates a rendering pass, and yellow an image-processing pass.)

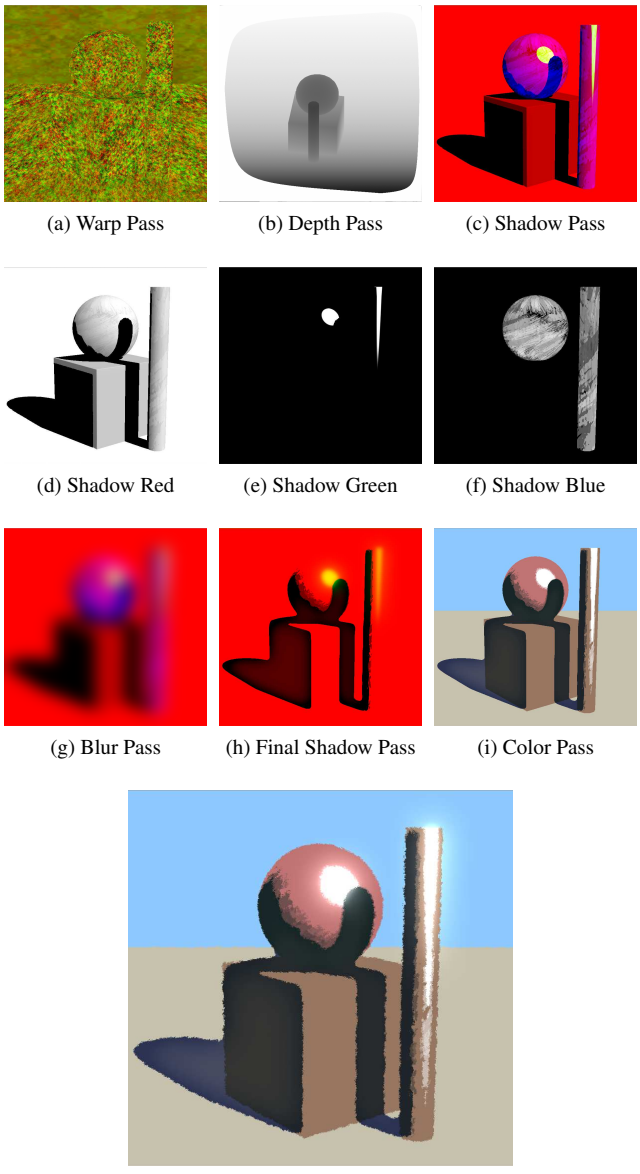

(a) Warp Pass (b) Depth Pass (c) Shadow Pass

(d) Shadow Red (e) Shadow Green (f) Shadow Blue

(g) Blur Pass (h) Final Shadow Pass (i) Color Pass

(j) Final Color Pass

Fig. 16: The various passes of our custom rendering pipeline.

Our pipeline consists of a series of 3D rendering passes interleaved with image-processing operations, as follows:

1. **Warp Pass** (render): In this pass we render all objects in the scene with the special shaders described in Section 4 (Figure 16a).
2. **Depth Pass** (render): Here we render only shadow-casting objects into a depth buffer, to be used later for casting shadows. The depth buffer's spatial coordinates are warped with a sigmoid function so as to provide more detail in the areas near the viewer (Figure 16b).
3. **Shadow Pass** (render): In this pass (Figure 16c) we render different information into each of the three channels (Figures 16d-16f). In the red channel, we render a simplified Lambert-shaded version of the objects, with cast shadows (Figure 16d). The green channel denotes objects that need to have screen-space lens effects, such as light sources or specular highlights (Figure 16e). We also apply an optional *breakup map* texture to the blue channel on certain surfaces (Figure 16f). This will be used later to control the "palette knife" effect for texture indication.
4. **Blur Pass** (image processing): Here we blur the Shadow Pass using a series of alternating 1D Gaussian blur and downsampling filters (Figure 16g).
5. **Final Shadow Pass** (image processing): In this pass we combine information from the Shadow Pass and Blur Pass to produce rounded shadow shapes, inner glow, and texture indication (Figure 16h). For details of how this is done, see Section 5.1.
6. **Color Pass** (render): In this pass we render the colors of all objects in the scene (Figure 16i), using the Final Shadow Pass as an input texture. For details, see Section 5.2.
7. **Final Color Pass** (image processing): In this final step of

the pipeline, we use the Warp Pass to warp the pixels of the Color Pass. (Here we also add bloom effects based on the Final Shadow Pass green channel.) (Figure 16j).

5.1. Shadow shapes, inner glow, and indication

To produce hard-edged silhouettes with rounded corners, we threshold the Blur Pass red channel. We create the Fuchs-inspired "inner glow" effect by inverting the Blur Pass and clamping it to add a bit of light to the interior of the dark regions. For texture indication, wherever the Shadow Pass blue channel is non-zero, we increase the number of steps in the thresholding operation. This has the effect of breaking up the transitions from light to shadow in regions of the surface that are oblique to the light direction (Figure 16h).

5.2. Color control

Each character and prop in the scene contains two full sets of texture maps, one for shadowed areas (Figure 17a), and one for illuminated areas (Figure 17b). These textures are hand-painted, and art-directed so that certain salient details may stand out only in shadows, and others only when lit. We use the Final Shadow Pass red channel to blend between these lit and shadowed texture maps on all objects.

(a) (b) (c)

Fig. 17: Texture examples: (a) shadow textures, (b) lit textures, (c) final result.

The shaders used in this pass also have color overlay and saturation controls, which can be used to adjust the coloring of the lit and shadowed regions independently, allowing us to achieve a variety of different lighting conditions and moods using only a few user controls. These controls are also animatable, allowing us to adjust lighting conditions smoothly over time.

6. Applications

Here are some examples of these techniques applied to the task of rendering characters and visual effects in *Age of Sail*.

6.1. Painterly Ocean

The ocean plays a critical role in the story of *Age of Sail*. The viewer's sense of peril hangs directly on the believability of this effect. The ocean also goes through significant transformations in texture, color and movement as the weather conditions change. To reproduce this complex natural phenomenon in a real-time experience, we rely on the strategy of removing unnecessary visual information.

In order to run on the full range of devices, the ocean's data footprint must be very small, and it cannot require excessive amounts of real-time computation. This excludes from consideration any approaches involving real-time fluid simulation, volumetric data, high resolution geometry, or overly long animation clips. We have focused on two key elements to present a convincing illusion: (1) realistic movement and wave silhouette shapes, and (2) a painterly appearance that suggests the infinite detail of the ocean using limited visual complexity, much the way Hoyne's paintings use brushstrokes of a limited thickness and palette.

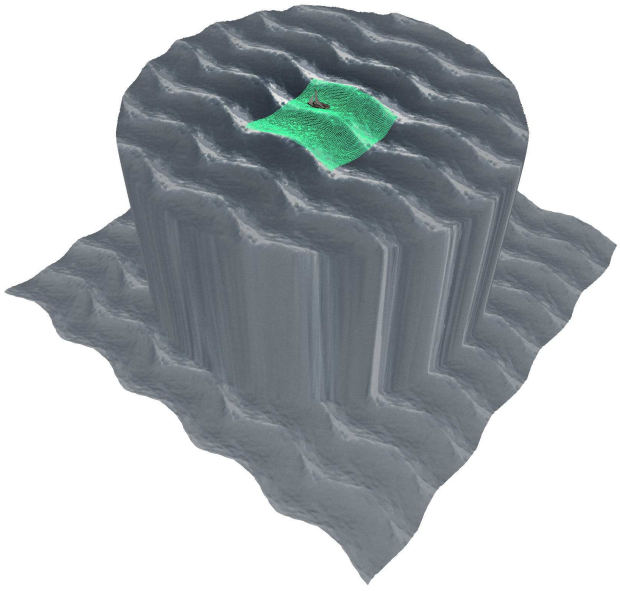

Fig. 18: The 5-by-5 grid of ocean tiles, with the center tile highlighted, and vertices pushed down beyond the "false horizon".

To capture the characteristic feeling of the shapes and movement of ocean waves, we use a Tessendorf deep ocean wave model [30]. This model has the advantage that it consists of waves that repeat periodically in both time and space. Thus we are able to apply this deformation to a very low-resolution mesh, an 80-by-80 square grid about 60 meters wide (approximately 75cm per quad in physical space), in a clip lasting 20 seconds, whose first and last frames match seamlessly. Because of the spatial repetition, one could tile an arbitrarily wide swath of ocean with instances of this single tile. However, since a typical human viewer cannot perceive distinctions in stereoscopic depth beyond about 50 meters, a 5-by-5 grid of these tiles turns out to be sufficient. To simulate travel across the ocean, we animate the tiles treadmill-style, translating them past the origin (where the boat remains, for the convenience of the animators) and allowing them to disappear behind the boat and reappear in front. We conceal this treadmilling action by using a vertex shader to push down vertices beyond a 120-meter radius "false horizon" (Figure 18), and use simpler geometry for the ring of ocean between that and the real horizon (about 1km away).

These ocean tiles are textured with a custom fragment shader to add detail only where it is needed (Figure 19e). The shader uses a hand-painted texture (Figure 19a) with MetaTexture to create an underlying dithering pattern that stays consistent in screen space regardless of viewpoint. This is then used as an in-

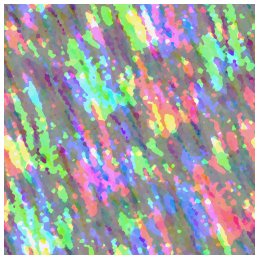

(a) Dithering

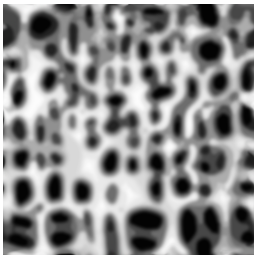

(c) Foam erosion

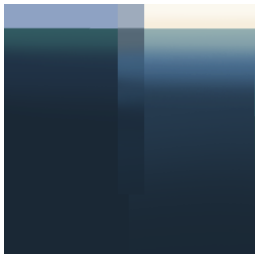

(b) Bathic map

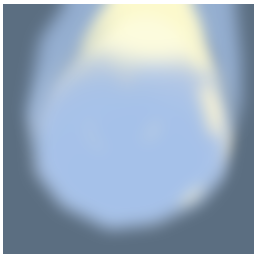

(d) Sky reflection

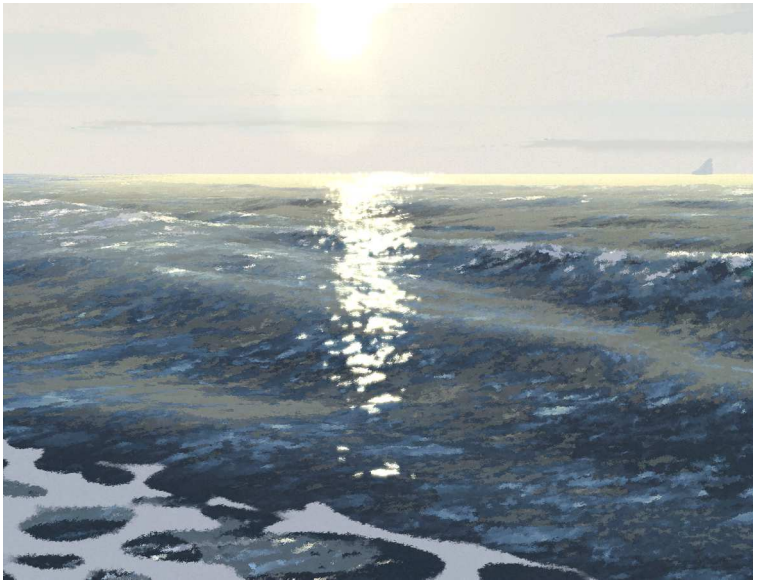

(e) The final rendered ocean.

Fig. 19: The various textures that contribute to the appearance of the ocean shader.

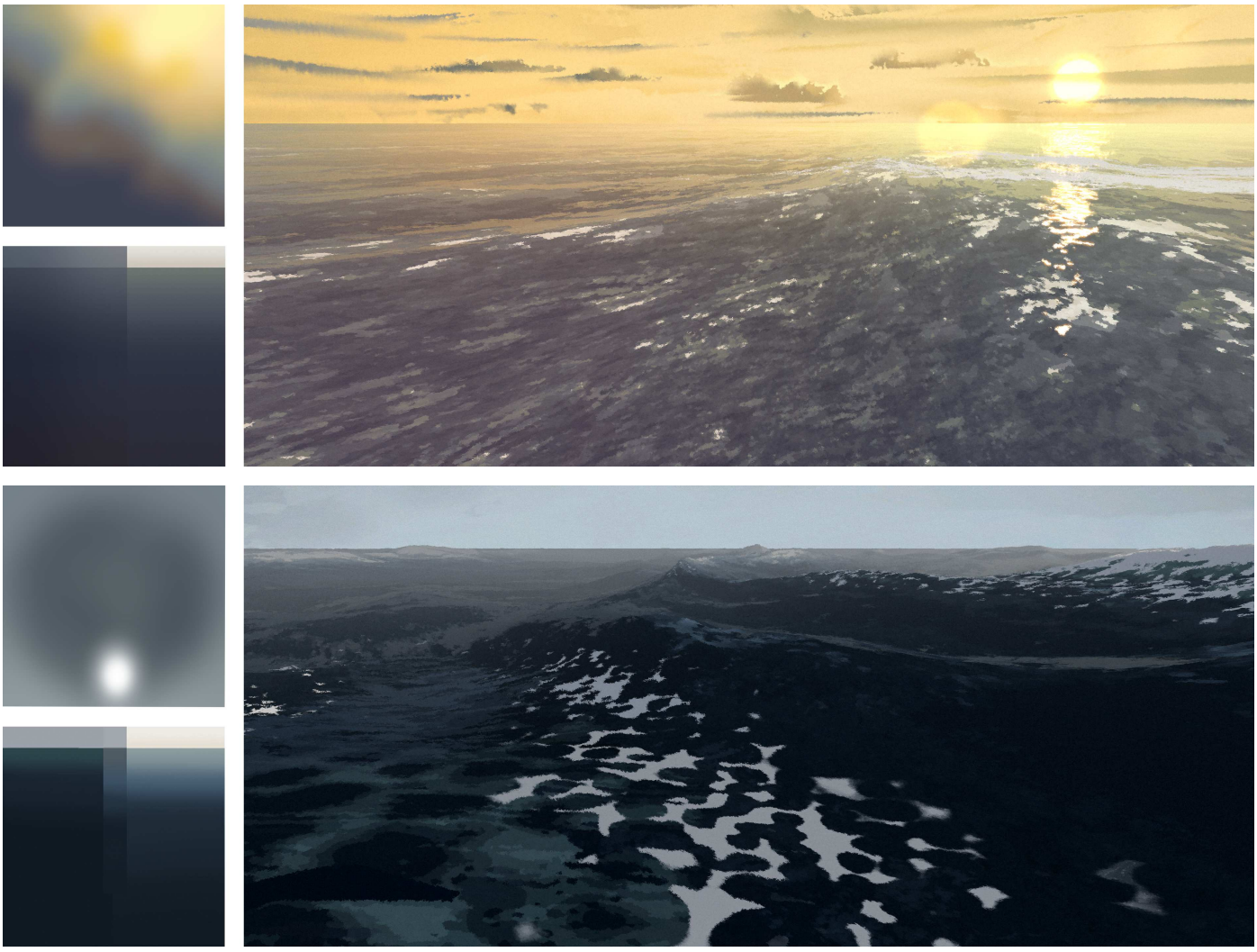

Fig. 20: Two other moments from *Age of Sail*, with their respective sky and bathic maps.

dex into a second texture, the *bathic map*, which represents the full palette of colors of the water at different depths and levels of illumination (Figure 19b.) Sea foam, based on a third texture (Figure 19c) is applied to the up-wind sides of the waves. A fourth texture acts as a sky reflection map (Figure 19d), which is also distorted using the dithering pattern. By changing the bathic and sky maps, we can create a variety of different moods (see Figure 20). In certain scenes we also apply animatable overlay color and saturation controls to each of these maps, to capture the gradual shift of colors due to changing weather conditions on the open sea.

The movement of the ocean geometry as it passes by the boat, combined with MetaTexture, creates a fairly dynamic effect when the viewer looks out towards the horizon. However, when looking directly down at a patch of ocean surface, sometimes the static nature of the dithering texture can become noticeable, breaking the subjective illusion of wateriness. To compensate for this, we calculate a "live texture" T' based on the original texture T, blending smoothly and cyclically through a mix of the red, green and blue channels at frequency f cycles per second (we have found frequencies between 0.5 and 1.0 to give pleasingly ocean-like results.)

$$\vec{T}' = \vec{L}_0 + (\vec{T} \cdot \vec{L}_1)\cos(ft) + (\vec{T} \cdot \vec{L}_2)\sin(ft) \tag{27}$$

where

$$\vec{L}_0 = \langle 0.5, 0.5, 0.5 \rangle \tag{28}$$

$$\vec{L}_1 = \langle 0.707, 0.0, -0.707 \rangle \tag{29}$$

$$\vec{L}_2 = \langle -0.408, 0.816, -0.408 \rangle \tag{30}$$

We can also offset the time value using world-space coordinates for an even more dynamic effect.

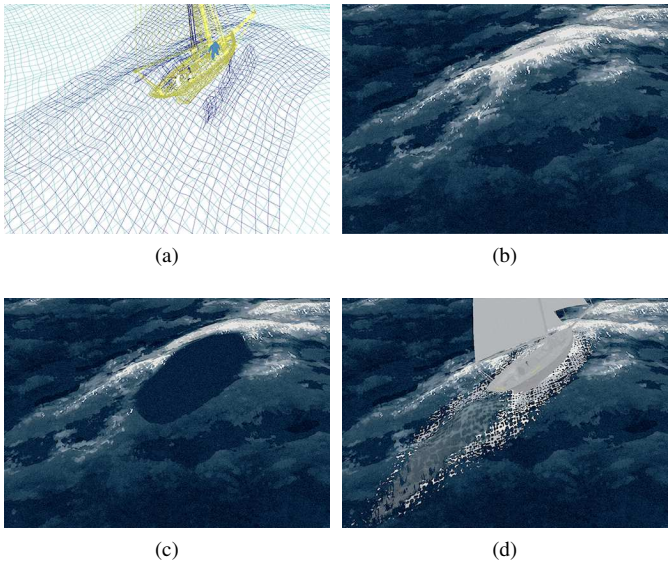

(a) (b) (c) (d)

Fig. 21: Decorating the ocean: (a) ocean, wake and splash geometry; (b) ocean surface; (c) ocean with vertices deformed and texture suppressed in the area around the boat; (d) wake superimposed seamlessly on top.

6.2. Wakes, ripples and splashes

Wherever a boat or character interacts with the ocean, more detailed movement is needed to produce a convincing effect. To achieve this, we *decorate* the ocean with smaller pieces of higher-resolution geometry for wakes, ripples and splashes (See Figure 21). To avoid geometry intersections and visually conflicting texture movement, we push the base mesh downwards, and suppress its texture so that it has effectively zero saliency (note that this is another case of removing information from the scene.)

Interestingly, if a partly transparent decoration is placed at the same height as the original ocean mesh, the holes in the decoration are not perceived as holes: because there are no salient details in the base mesh's texture, its color appears to become part of the decoration's texture. The result, even in stereoscopic 6DoF VR, is the illusion of a perfectly seamless ocean.

6.3. Animated Characters

Another area where we have deliberately removed information is in the character animation. The characters in *Age of Sail* were animated at 24fps, on "twos and threes" i.e. with poses held static for 2-3 frames (83-125ms) rather than smoothly interpolated between keys. The characters also have animated line boil to keep them alive even when they are not moving. In combination, these two effects support the feeling that the animation is hand-crafted as opposed to synthetic. We also reduced the intensity of the edge breakup on facial features to keep their expressions clear (Figure 22), and on entire characters when they are far from camera (Figure 14b).

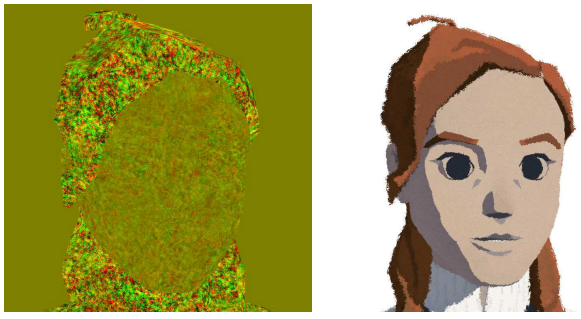

(a) (b)

Fig. 22: Reduced edge breakup on facial features.

7. Discussion

New developments in entertainment media technology often lead to a shift in audience response. For example, the release of the first high frame rate (48fps) stereoscopic film *The Hobbit* had a polarizing effect on the audience: while most viewers enjoyed the added realism, for some the high frame rate made the artifice of prosthetics, sets and synthetic characters too obvious when juxtaposed against the real human actors, a dissonance that prevented them from suspending their disbelief [31].

We suspect that virtual reality may have its own version of the Uncanny Valley [32]: as a simulation's information density

increases, so does our ability to detect fakery within it. Since VR devices, with their high frame rates and interactive responsiveness, have an inherently high information density, staying on the right side of this "Unbelievable Valley" would require a level of realism unachievable with current hardware. We chose instead to run to the left. By simplifying the visual style and choosing a deliberately staccato frame rate, we seem to have reduced the information density enough to compensate for the device's excesses.

7.1. Taking the Art Seriously

We feel we were largely successful in capturing the concept art's important qualities (Figures 1-3) in the final rendered results (Figure 4). This is not so much because of a particular graphics technique, but because of the structure of our collaboration. The key is *taking the concept art seriously*: if production designers create paintings that truly represent how they envision the end product, and graphics developers seek to understand the concept art's details deeply enough to adapt them to a new medium, and each group asks thoughtful questions about the other's creative process, and answers them openly, this cycle of feedback inevitably leads to good results. We hope this work serves as a positive example of how artists and engineers can collaborate effectively in any medium.

7.2. Performance

Age of Sail runs in real time on devices ranging from tethered VR headsets to mobile phones. It renders an average of 800,000 triangles grouped into approximately 250 meshes, at a consistent frame rate of 90fps on a Windows 10 PC with an NVidia GeForce GTX1080 GPU. On mobile hardware such as a Pixel 3 or iPhone 8, it plays consistently at 57-60fps in both mono- and stereoscopic modes.

7.3. Limitations

These techniques are certainly applicable to a wide variety of other visual styles beyond that of *Age of Sail*. However, there are certain limitations that should be considered.

The edge breakup can produce a noticeable "heat ripple" effect, where a foreground object's warp field distorts the background in the area immediately around it, if the background has a lot of salient, high-contrast detail (Figure 23). In such circumstances it may be preferable to render and warp the scene in multiple layers, although that would come at a higher computational cost.

7.4. Future Work

This project raises some questions that warrant further study. For example, is there an ideal frame rate for animated characters in an immersive medium? Our choice to animate the characters "on twos" (12fps) was deliberate, and has been well received by most viewers, but there is a segment of our audience who find that frame rate distracting. It would be interesting to explore this further via a control experiment or survey similar to Michelle et al [31].

We also note that our choice to use powers of two as our discrete set of scale values for our implementation of MetaTexture,

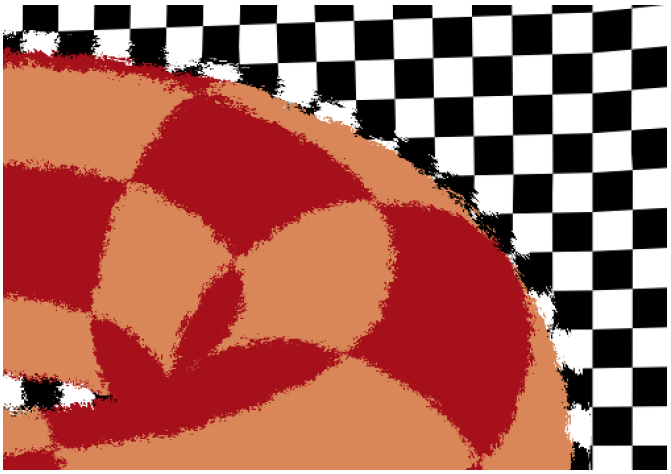

Fig. 23: "Heat ripple" effect (exaggerated here for clarity). Note that the black and white checkered background is distorted near the edges of the red torus.

although entirely natural for those familiar with graphics techniques like mipmaps, is somewhat arbitrary. It may be possible to get different and interesting results by quantizing based on powers of some other number, such as 3, $\sqrt{2}$ or the golden ratio ϕ. Also, texture orientation need not remain the same from one scale level to the next. Our skew compensation method works well enough in practice, but is admittedly *ad hoc*, and there may be more robust approaches that we have not yet considered. One can think of our particular implementation of MetaTexture as a subset of a much larger space of possible example-based texturing techniques that differ in their details while retaining the same core principle of balancing screen-space texture scale against stereoscopic 3D coherence. We would like to explore that space further.

Our early experiments using these techniques in augmented reality (see Figure 24) also raise interesting questions: how should stylized virtual characters integrate into a real-world background, and how can that background be manipulated to feel consistent with the visual style?

Fig. 24: A scene from augmented reality experiment *The End*.

8. Acknowledgements

The authors would like to thank: Dan Kaufman for his support of our efforts, Rachid El Guerrab for asking an interesting question four years ago, Jan Pinkava, Karen Dufilho, and David Eisenmann for their unwavering leadership, Céline Desrumaux and Jasmin Lai for their inspiring production design, Josiah Larson for sweating the details, Tim J. Smith for

psychological insights, Jon Klassen for designing and directing *The End*, David Apatoff and the Fuchs family for sharing Bernie Fuchs' work, and everyone at Google ATAP, Chromosphere LA, Boathouse Studios and Evil Eye Pictures for their contributions to *Age of Sail*.

References

[1] Kahrs, J. Age of Sail. https://atap.google.com/spotlight-stories/age-of-sail/; 2018.

[2] Kalnins, RD, Davidson, PL, Markosian, L, Finkelstein, A. Coherent stylized silhouettes. In: ACM SIGGRAPH 2003 Papers. SIGGRAPH '03; New York, NY, USA: ACM. ISBN 1-58113-709-5; 2003, p. 856–861. doi:10.1145/1201775.882355.

[3] Zheng, M, Milliez, A, Gross, M, Sumner, RW. Example-based brushes for coherent stylized renderings. In: Proceedings of the Symposium on Non-Photorealistic Animation and Rendering. NPAR '17; New York, NY, USA: ACM. ISBN 978-1-4503-5081-5; 2017, p. 3:1–3:10. doi:10.1145/3092919.3092929.

[4] Bénard, P, Cole, F, Kass, M, Mordatch, I, Hegarty, J, Senn, MS, et al. Stylizing animation by example. ACM Trans Graph 2013;32(4):119:1–119:12. doi:10.1145/2461912.2461929.

[5] Bénard, P, Cole, F, Golovinskiy, A, Finkelstein, A. Self-similar texture for coherent line stylization. In: Proceedings of the 8th International Symposium on Non-Photorealistic Animation and Rendering. NPAR '10; New York, NY, USA: ACM. ISBN 978-1-4503-0125-1; 2010, p. 91–97. doi:10.1145/1809939.1809950.

[6] Bléron, A, Vergne, R, Hurtut, T, Thollot, J. Motion-coherent stylization with screen-space image filters. In: Proceedings of the Joint Symposium on Computational Aesthetics and Sketch-Based Interfaces and Modeling and Non-Photorealistic Animation and Rendering. Expressive '18; New York, NY, USA: ACM. ISBN 978-1-4503-5892-7; 2018, p. 10:1–10:13. doi:10.1145/3229147.3229163.

[7] Bénard, P, Lagae, A, Vangorp, P, Lefebvre, S, Drettakis, G, Thollot, J. A dynamic noise primitive for coherent stylization. In: Proceedings of the 21st Eurographics Conference on Rendering. EGSR'10; Aire-la-Ville, Switzerland, Switzerland: Eurographics Association; 2010, p. 1497–1506. doi:10.1111/j.1467-8659.2010.01747.x.

[8] Bénard, P, Bousseau, A, Thollot, J. Dynamic solid textures for real-time coherent stylization. In: Proceedings of the 2009 Symposium on Interactive 3D Graphics and Games. I3D '09; New York, NY, USA: ACM. ISBN 978-1-60558-429-4; 2009, p. 121–127. doi:10.1145/1507149.1507169.

[9] Whited, B, Daniels, E, Kaschalk, M, Osborne, P, Odermatt, K. Computer-assisted animation of line and paint in Disney's Paperman. In: ACM SIGGRAPH 2012 Talks. SIGGRAPH '12; New York, NY, USA: ACM. ISBN 978-1-4503-1683-5; 2012, p. 19:1–19:1. doi:10.1145/2343045.2343071.

[10] Kass, M, Pesare, D. Coherent noise for non-photorealistic rendering. In: ACM SIGGRAPH 2011 Papers. SIGGRAPH '11; New York, NY, USA: ACM. ISBN 978-1-4503-0943-1; 2011, p. 30:1–30:6. doi:10.1145/1964921.1964925.

[11] Klein, AW, Li, W, Kazhdan, MM, Corrêa, WT, Finkelstein, A, Funkhouser, TA. Non-photorealistic virtual environments. In: Proceedings of the 27th Annual Conference on Computer Graphics and Interactive Techniques. SIGGRAPH '00; New York, NY, USA: ACM Press/Addison-Wesley Publishing Co. ISBN 1-58113-208-5; 2000, p. 527–534. doi:10.1145/344779.345075.

[12] Haller, M, Sperl, D. Real-time painterly rendering for MR applications. In: Proceedings of the 2nd International Conference on Computer Graphics and Interactive Techniques in Australasia and South East Asia. GRAPHITE '04; New York, NY, USA: ACM. ISBN 1-58113-883-0; 2004, p. 30–38. doi:10.1145/988834.988839.

[13] Haller, M, Landerl, F, Billinghurst, M. A loose and sketchy approach in a mediated reality environment. In: Proceedings of the 3rd International Conference on Computer Graphics and Interactive Techniques in Australasia and South East Asia. GRAPHITE '05; New York, NY, USA: ACM. ISBN 1-59593-201-1; 2005, p. 371–379. doi:10.1145/1101389.1101463.

[14] Chen, J, Turk, G, MacIntyre, B. Watercolor inspired non-photorealistic rendering for augmented reality. In: Proceedings of the 2008 ACM Symposium on Virtual Reality Software and Technology. VRST '08; New York, NY, USA: ACM. ISBN 978-1-59593-951-7; 2008, p. 231–234. doi:10.1145/1450579.1450629.

[15] Fischer, J, Bartz, D, Strasser, W. Artistic reality: Fast brush stroke stylization for augmented reality. In: Proceedings of the ACM Symposium on Virtual Reality Software and Technology. VRST '05; New York, NY, USA: ACM. ISBN 1-59593-098-1; 2005, p. 155–158. doi:10.1145/1101616.1101649.

[16] Northam, L, Asente, P, Kaplan, CS. Consistent stylization and painterly rendering of stereoscopic 3d images. In: Proceedings of the Symposium on Non-Photorealistic Animation and Rendering. NPAR '12; Goslar Germany, Germany: Eurographics Association. ISBN 978-3-905673-90-6; 2012, p. 47–56.

[17] Saito, T, Takahashi, T. Comprehensible rendering of 3-d shapes. In: Proceedings of the 17th Annual Conference on Computer Graphics and Interactive Techniques. SIGGRAPH '90; New York, NY, USA: ACM. ISBN 0-89791-344-2; 1990, p. 197–206. doi:10.1145/97879.97901.

[18] Bénard, P, Lu, J, Cole, F, Finkelstein, A, Thollot, J. Active strokes: Coherent line stylization for animated 3D models. In: Proceedings of the Symposium on Non-Photorealistic Animation and Rendering. NPAR '12; Goslar Germany, Germany: Eurographics Association. ISBN 978-3-905673-90-6; 2012, p. 37–46. URL: http://dl.acm.org/citation.cfm?id=2330147.2330156.

[19] Dirksen, N. Creating a VR storybook look for Rainbow Crow. https://www.youtube.com/watch?v=uELM5qQvBkY; 2017.

[20] Curtis, C, Eisenmann, D, El Guerrab, R, Stafford, S. The making of "Pearl", a 360° Google Spotlight Story. In: ACM SIGGRAPH 2016 VR Village. SIGGRAPH '16; New York, NY, USA: ACM. ISBN 978-1-4503-4377-0; 2016, p. 21:1–21:1. doi:10.1145/2929490.2956565.

[21] Curtis, C. Non-photorealistic animation. ACM SIGGRAPH 1999 Course Notes 1999;17.

[22] Curtis, CJ, Dart, K, Latzko, T, Kahrs, J. Non-Photorealistic Animation for Immersive Storytelling. In: ACM/EG Expressive Symposium. The Eurographics Association. ISBN 978-3-03868-078-9; 2019,doi:10.2312/exp.20191071.

[23] Apatoff, D. The Life and Art of Bernie Fuchs. The Illustrated Press; 2017. ISBN 0997029269.

[24] Palley, R, Palley, MA. Wooden Ships and Iron Men: The Maritime Art of Thomas Hoyne. Quantuck Lane Press; 2005. ISBN 1593720130.

[25] Winkenbach, G, Salesin, DH. Computer-generated pen-and-ink illustration. In: Proceedings of the 21st Annual Conference on Computer Graphics and Interactive Techniques. SIGGRAPH '94; New York, NY, USA: ACM. ISBN 0-89791-667-0; 1994, p. 91–100. doi:10.1145/192161.192184.

[26] Reid, C. Planning lost and found edges. Watercolor Artist Magazine 2009;.

[27] Barzel, R, Hughes, JR, Wood, DN. Plausible motion simulation for computer graphics animation. In: Boulic, R, Hégron, G, editors. Computer Animation and Simulation '96. Vienna: Springer Vienna. ISBN 978-3-7091-7486-9; 1996, p. 183–197.

[28] Bénard, P, Thollot, J, Sillion, F. Quality assessment of fractalized NPR textures: A perceptual objective metric. In: Proceedings of the 6th Symposium on Applied Perception in Graphics and Visualization. APGV '09; New York, NY, USA: ACM. ISBN 978-1-60558-743-1; 2009, p. 117–120. doi:10.1145/1620993.1621016.

[29] Heitz, E, Neyret, F. High-performance by-example noise using a histogram-preserving blending operator. Proc ACM Comput Graph Interact Tech 2018;1(2):31:1–31:25. doi:10.1145/3233304.

[30] Tessendorf, J. Simulating ocean surfaces. ACM SIGGRAPH 2004 Course Notes 2004;32.

[31] Michelle, C, Davis, C, Hight, C, Hardy, A. The Hobbit hyperreality paradox: Polarization among audiences for a 3D high frame rate film. Convergence: The International Journal of Research into New Media Technologies 2015;23. doi:10.1177/1354856515584880.

[32] Mori, M, MacDorman, KF, Kageki, N. The uncanny valley [from the field]. IEEE Robotics Automation Magazine 2012;19(2):98–100. doi:10.1109/MRA.2012.2192811.